Journal of Civil Engineering and Architecture 20 (2026) 385-399
doi: 10.17265/1934-7359/2026.09.003

Morphology of the Deformation Curve of Elastoplastic Materials

P. A. Belov[1], N. Ya. Golovina[2] and Elliot Weiss[3]

1. Institute of Applied Mechanics of the Russian Academy of Sciences, Moscow 125040, Russia

2. Industrial University of Tyumen (IUT), Surgut Branch, Surgut 628400, Tyumen Region, Russia

3. Independent Researcher, USA

Abstract: A hierarchical variational generalization of the Reinsch principle is proposed for constructing an adaptive interpolation-spline architecture from a finite experimental sample of the deformation curve of an elastoplastic material. The approach separates three interrelated levels. At the first level, stationarity of the integral part of the variational functional determines the admissible structure of local solutions, including their fundamental functions and variationally consistent boundary and contact conditions. The C^2class is adopted as the preferred maximum local smoothness class, while information-insufficient segments are represented by the highest admissible lower class according to the hierarchy $C^2 \to C^1 \to C^0$. At the second level, for each fixed architecture, minimization of the discrete part determines the phenotypic coefficients of the local fundamental solutions from the experimental sample. At the third level, DOE (Design of Experiments) is used to organize and compare the successive architectural states of the deterministic genealogy generated by Geometry Builder; no global search over all admissible spline architectures is performed. The genealogical construction starts from a full-range C^2model and develops through greedy multiplication. At each iteration, the segment containing the experimental point of the global maximum Euclidean point-to-curve defect is selected as the parent segment. This point becomes the mandatory new internal boundary and the common experimental point of the two child segments. Their highest admissible local classes are determined by information capacity, whereas insufficient approximation accuracy leads to subsequent multiplication rather than artificial reduction of the local class. Previously accepted boundaries are neither relocated nor removed, so the architecture evolves monotonically. Construction terminates either when both the distributed root-mean-square tolerance and the geometric point-to-curve tolerance are satisfied or when no further information-supported multiplication is possible and the information limit is reached. The terminal morphology is defined exclusively by the number of spline segments and the coordinates of their internal boundaries and is therefore distinguished from the complete computational architecture, which additionally contains local smoothness classes, fundamental solutions, phenotypic coefficients, and boundary and contact conditions. A theorem on morphological stability is formulated, and numerical examples demonstrate automatic construction of different deformation-curve morphologies without prescribing the number of segments in advance. The resulting morphology constitutes an independent geometric result and a fixed basis for the subsequent construction of an approximation template and identification of physical material parameters by the Material Builder module within the Computational Platform for Machine Recognition of Elastoplastic Materials.

Key words: Material genetics, deformation-curve morphology, interpolation template, adaptive spline, full-range model, greedy multiplication, Reinsch principle, morphological stability, dual accuracy control, information limit.

1. Introduction

A geometric representation of an experimental deformation curve by a spline is commonly constructed with a preselected number of segments or knots. Such a choice effectively prescribes the model architecture before analysis of the experimental sample and may therefore conflate two distinct problems: determination of a geometrically sufficient structure for representing the curve and subsequent identification of the physical properties of the material.

Corresponding author: Petr A. Belov, D.Sc. (Phys.-Math.), Leading Researcher, research fields: mechanics of materials, constitutive modeling, inverse problems, materials genetics.

In the present work these problems are separated. First, a geometrically sufficient architecture of the interpolation spline is constructed from a finite experimental sample and the morphology of the deformation curve is determined. Physical identification of the material is performed at the next stage and lies outside the scope of the present paper. This separation continues the systematic development of the genetics of elastoplastic materials and of the direct and inverse problem formulations introduced in previous works [1-4].

The basis of the geometric construction is the hierarchical variational generalization of the Reinsch principle proposed in this work [5]. In contrast to the traditional formulation, the variational and discrete components of the problem perform different functions. Stationarity of the integral part determines the space of fundamental solutions of a prescribed local class together with the corresponding boundary and contact conditions. For a fixed architecture, minimization of the discrete part determines the phenotypic coefficients that provide its optimal agreement with the experimental sample. Thus, the variational construction determines not only a particular interpolation function but also the mathematically admissible structure within which its phenotypic identification is performed.

The starting basis of the construction is the full-range model of class C^2 occupying the entire working strain domain. If it does not provide the prescribed accuracy, the architecture develops through greedy multiplication. At each step, the parent is the segment containing the experimental point of the global maximum Euclidean point-to-curve defect; this point becomes the mandatory new internal boundary of the two child segments. Their highest admissible local classes are determined by information capacity. Consequently, neither the number of segments nor the positions of their boundaries or the sequence of local classes are prescribed in advance; they arise during the genealogical development of the architecture.

This construction also extends the role of DOE (Design of Experiments). In a conventional parametric formulation, DOE organizes variation of model parameters for a fixed structure. In the proposed construction, the admissible spline architectures and structures themselves become objects of systematic variation and comparison, each possessing its own optimally identified phenotypic realization. DOE thereby provides a framework for investigating architectural variations, whereas Geometry Builder supplies the deterministic mechanism by which these variations are generated.

Architecture and morphology of the interpolation template must be distinguished. Architecture is the complete computational state of the model and includes the segmentation, local classes, fundamental solutions, phenotypic coefficients, and boundary and contact conditions. Morphology is the terminal geometric characteristic of this architecture and is defined only by the number of segments and the coordinates of their internal boundaries. Different computational architectures may therefore correspond to the same morphology.

The objective of the present work is to develop and computationally verify a hierarchical variational method for constructing an adaptive interpolation-spline architecture—from the full-range model through greedy multiplication, information-based selection of local classes, and phenotypic identification to an automatically determined morphology of the deformation curve. Construction terminates either when the prescribed dual accuracy is reached or when the information limit of the experimental sample is attained. The resulting morphology is treated as an independent geometric result and simultaneously as a fixed basis for the next stage in the development of the Computational Platform for Machine Recognition of Elastoplastic Materials: construction of an approximation template and identification of the physical parameters of the material by means of the additional Material Builder module.

2. Hierarchical Variational Construction of a Variable-Architecture Interpolation Template

Let the working experimental sample of the deformation

curve after preprocessing be represented by the ordered set

$$\mathcal{D} = \{(\varepsilon_k, \sigma_k)\}_{k=1}^{N} \quad (1)$$

Geometry Builder constructs from this sample a composite interpolation spline with an a priori unknown number of segments, unknown positions of internal boundaries, and variable local smoothness classes. The class C^2 is adopted as the preferred maximum local class, whereas C^1 and C^0 are used when the information capacity of the corresponding segment is insufficient for a higher-class representation.

Architecture and morphology of the spline must be distinguished. The architecture $\mathcal{A}$ characterizes the complete current mathematical state of the model and includes the number and boundaries of segments, their local classes, fundamental solutions, boundary and contact conditions, and phenotypic coefficients. Morphology is the geometric projection of the architecture,

$$\mathcal{M} = \{m; \varepsilon_1, \dots, \varepsilon_{m-1}\} \quad (2)$$

where m is the number of segments and ε_i are the coordinates of internal boundaries. Thus, a change in local class or phenotypic coefficients with all boundaries fixed changes the architecture but not the morphology.

The construction is hierarchical. First, the variational principle determines the admissible structure of local solutions. The full-range model is then constructed as the initial element of the architecture. Subsequent greedy multiplication of segments changes the spline architecture; information capacity determines the admissible classes of child segments; and, for each fixed architecture, the phenotypic coefficients are determined by minimization of the discrete part of the functional. The resulting sequence of architectures forms a family of structural variants whose systematic investigation is naturally formulated in terms of DOE.

2.1 Hierarchical Variational Generalization of the Reinsch Principle

In the classical Reinsch construction, smoothness of a spline representation is controlled by an integral measure of derivative variation together with a measure of discrepancy from experimental data [5]. In the present generalization, these two components have different functions: the integral part determines the structure of the admissible solution space, whereas the discrete part determines the phenotypic coefficients of a particular representative of this space.

For a local segment of class C^q, $q = 0,1,2$, consider the integral functional

$$\mathcal{I}_q[\sigma] = \int_{\Omega} \left[\sigma^{(q+1)}(\varepsilon)\right]^2 \, d\varepsilon \quad (3)$$

Its stationarity condition is

$$\delta \mathcal{I}_q = 0 \quad (4)$$

After $q+1$ integrations by parts, the Euler equation inside the segment is

$$\sigma^{(2q+2)} = 0) \quad (5)$$

Consequently, the local space of fundamental solutions has dimension $2q+2$, and its polynomial basis has maximum degree

$$p_q = 2q + 1 \quad (6)$$

This gives the unified variational hierarchy

$$\begin{aligned} C^0&: \ \sigma'' = 0, \ p_0 = 1 \\ C^1&: \ \sigma^{(4)} = 0, \ p_1 = 3 \\ C^2&: \ \sigma^{(6)} = 0, \ p_2 = 5 \end{aligned} \quad (7)$$

Thus, linear, cubic, and quintic local segments are not introduced as independent empirical models. They are fundamental solutions of the same variational construction for different admissible smoothness classes.

The first variation of the integral part also contains boundary terms. At external boundaries, together with prescribed essential conditions, these terms determine the corresponding natural boundary conditions. When the domain is divided into segments, the boundary terms of adjacent segments, together with the required continuity, determine their contact conditions. Hence,

$$\begin{aligned} \delta \mathcal{I}_q = 0 \ \Rightarrow \ \{&\text{fundamental solutions;} \\ &\text{boundary conditions;} \\ &\text{contact conditions}\} \end{aligned} \quad (8)$$

The integral part therefore determines the variationally admissible structure of a local spline but

does not identify the phenotypic coefficients from the experimental sample. This constitutes the first level of the hierarchical variational generalization of the Reinsch principle.

2.2 Full-Range Model as the Initial Element of the Architecture

The initial architecture of Geometry Builder consists of a single segment occupying the entire working domain $\Omega_0 = [0,1]$. The preferred maximum class C^2 is assigned to this segment. Therefore,

$$\sigma^{(6)} = 0 \tag{9}$$

and the fundamental basis is

$$\{1, \varepsilon, \varepsilon^2, \varepsilon^3, \varepsilon^4, \varepsilon^5\}) \tag{10}$$

Accordingly, the full-range solution is represented as the linear combination

$$\sigma_{FR}(\varepsilon) = c_0 + c_1\varepsilon + c_2\varepsilon^2 + c_3\varepsilon^3 + c_4\varepsilon^4 + c_5\varepsilon^5 = \sum_{j=0}^{5} c_j\, \varepsilon^j \tag{11}$$

where the coefficient vector $\mathbf{c}_{FR} = (c_0, c_1, \dots, c_5)^T$ is the phenotype of the full-range segment. More generally, the coefficients of the linear combination of the fundamental solutions of any segment constitute the phenotype of that segment. The variational construction determines the admissible basis and boundary/contact structure, whereas the numerical phenotype is identified from the discrete experimental data.

At the left external boundary, the essential conditions are $\sigma(0) = 0$ and $\sigma''(0) = 0$, while the corresponding free variation yields the natural condition $\sigma^{(4)}(0) = 0$. At the right external boundary, the essential conditions are $\sigma(1) = 1$ and $\sigma'(1) = 0$, while the free variation yields the natural condition $\sigma'''(1) = 0$. Thus,

$$\sigma(0) = 0, \qquad \sigma''(0) = 0, \qquad \sigma^{(4)}(0) = 0, \tag{12}$$

$$\sigma(1) = 1, \qquad \sigma'(1) = 0, \qquad \sigma'''(1) = 0. \tag{13}$$

Equation (9), basis (10), representation (11), and conditions (12)-(13) uniquely define the C^2 full-range model as the initial structural element of the architecture. This structural definition must not be confused with identification of the numerical phenotype $\mathbf{c}_{FR}$ of a particular material, which is performed from the experimental sample by the discrete part of the problem.

The full-range model represents the starting basis for the subsequent genealogical construction,

$$\mathcal{A}_0 = \{\text{full-range } C^2 \text{ model}\} \tag{14}$$

2.3 Greedy Multiplication of the Parent Segment

For every current architecture, after identification of its phenotypic coefficients, the governing local discrepancy at an experimental point P_k=(ε̄_k,σ̄_k) is the Euclidean point-to-curve distance to the current local spline segment S_{j(k)} containing the abscissa ε̄_k:

$$d_k = min_\{Q \in S_\{j(k)\}\} \ \|P_k - Q\|_2 \tag{15}$$

The accuracy of the current spline is controlled by two complementary measures: the conventional vertical root-mean-square error E_RMS, which characterizes the distributed discrepancy over the sample, and the maximum Euclidean point-to-curve defect D_max, which controls the strongest local geometric discrepancy. Their explicit definitions and distinct tolerances are given in Section 2.7.

If this dual accuracy criterion is not satisfied, the experimental point with the global maximum Euclidean point-to-curve defect is determined:

$$k* = arg\ \ max_k\ \ d_k \tag{16}$$

Let

$$P_* = (\varepsilon_*, \sigma_*), \qquad \varepsilon_* = \varepsilon_{k_*}, \qquad \sigma_* = \sigma_{k_*}. \tag{17}$$

The point P_* performs three functions simultaneously: it identifies the parent segment, fixes the position of the mandatory new internal boundary, and becomes the common experimental point through which both child segments must pass.

Let the parent segment occupy $\Omega_p = [a, b]$, with $a < \varepsilon_* < b$. Greedy multiplication replaces it by

$$\Omega_L = [a, \varepsilon_*], \qquad \Omega_R = [\varepsilon_*, b], \tag{18}$$

with

$$\sigma_L(\varepsilon_*) = \sigma_R(\varepsilon_*) = \sigma_* \tag{19}$$

The new boundary is therefore neither an additional continuous optimization variable nor a point selected from a candidate window; it is uniquely fixed by the current global maximum of the interpolation error.

Before assigning classes to the children, information capacity is understood as the number of experimental points available on a segment relative to the number of independent coefficients required by the lowest-degree fundamental polynomial of a given local class. A child is assigned the highest class for which this information requirement is satisfied. The quantitative capacities $C^2: 6$, $C^1: 4$, and $C^0: 2$ points and the corresponding parent capacities are derived in Section 2.4. Thus, information capacity determines admissible class, whereas approximation error determines whether further multiplication is required.

After the child classes have been selected, the variational construction (3)-(8) supplies their fundamental solutions and admissible boundary/contact conditions. The phenotypic coefficients of the rebuilt local block are then reidentified from the experimental sample. Four structurally different multiplication cases must be distinguished.

2.3.1 Multiplication of the Full-Range Model

The first multiplication is a special case because the only initial segment is simultaneously the left and right extreme segment: $a = 0,\ b = 1$. Hence,

$$[0,1] \to [0, \varepsilon_*] \cup [\varepsilon_*, 1] \tag{20}$$

The left child inherits the variationally admissible global left boundary conditions compatible with its information-admissible local class. The right child analogously inherits the global right boundary conditions. At the new internal boundary ε_*, contact conditions between the two children arise for the first time, and both children pass through P_*. This first multiplication produces the transition

$$\text{full-range model} \to \text{composite spline} \tag{21}$$

2.3.2 Multiplication of an Internal Parent Segment

If $0 < a < \varepsilon_* < b < 1$, the parent is internal. Its external block boundaries a and b remain fixed. At these boundaries the children inherit the already established contact conditions of the current architecture to the extent compatible with their new local classes. A new boundary ε_* is introduced inside the block,

$$[a, b] \to [a, \varepsilon_*] \cup [\varepsilon_*, b] \tag{22}$$

All segments and boundaries outside $[a, b]$ remain unchanged. Multiplication is therefore a local operation on the architecture.

2.3.3 Multiplication of the Left Extreme Parent Segment

If $a = 0$ and $b < 1$, the parent is the left extreme segment:

$$[0, b] \to [0, \varepsilon_*] \cup [\varepsilon_*, b] \tag{23}$$

The left child inherits the global left boundary conditions admissible for its local class. New contact conditions are formed at ε_*. At b, the right child inherits the contact conditions with the unchanged part of the current spline. Thus, the global left boundary retains its status while one new internal boundary is introduced inside the parent segment.

2.3.4 Multiplication of the Right Extreme Parent Segment

If $0 < a$ and $b = 1$, the parent is the right extreme segment:

$$[a, 1] \to [a, \varepsilon_*] \cup [\varepsilon_*, 1] \tag{24}$$

At a, the left child inherits the contact conditions with the unchanged part of the spline. New contact conditions arise at ε_*. The right child inherits the variationally admissible global right boundary conditions compatible with its local class.

All four cases obey the common genealogical law

$$\text{parent} \to \{\text{left child,right child}\} \tag{25}$$

They differ only in the inheritance of the external conditions of the rebuilt block. The greedy character of the algorithm means that at every step the segment containing the global maximum of the current Euclidean point-to-curve defect is multiplied. Greedy multiplication is therefore the sequential local multiplication of the segment containing the strongest current discrepancy between the interpolation template and the experimental sample.

2.4 Information Capacity and Classes of Child Segments

From (6), the number of coefficients of a local fundamental solution of class C^q is

$$N_{\min}^{(q)} = p_q + 1 = 2(q+1), \qquad q = 0,1,2. \quad (26)$$

Therefore,

$$C^2\colon N_{\min}^{(2)} = 6; \qquad C^1\colon N_{\min}^{(1)} = 4; \qquad C^0\colon N_{\min}^{(0)} = 2. \quad (27)$$

Once the mandatory boundary position has been fixed by (16), each child is assigned the highest information-admissible class,

$$q(N) = \begin{cases} 2, & N \geq 6, \\ 1, & 4 \leq N < 6, \\ 0, & 2 \leq N < 4. \end{cases} \quad (28)$$

Because the experimental split point P_* belongs to both children, the minimum number of distinct experimental points required in a parent for a prescribed pair of child classes is

$$N_{\min}^{(q_L,q_R)} = N_{\min}^{(q_L)} + N_{\min}^{(q_R)} - 1 \quad (29)$$

Hence the minimum parent capacities for C^2/C^2, C^2/C^1, C^2/C^0, C^1/C^1, C^1/C^0, and C^0/C^0 are respectively 11, 9, 7, 7, 5, and 3 distinct experimental points.

For a complete architecture containing m_0, m_1, and m_2 segments of classes C^0, C^1, and C^2, respectively, the same counting principle gives a global lower estimate for the number N of distinct experimental sample points required to support that architecture. Each first segment requires its full local capacity, whereas every subsequent segment shares one boundary sample point with the already constructed part of the spline. Therefore,

$$N \geq m_0 + 3m_1 + 5m_2 + 1 \quad (29a)$$

The right-hand side of (29a) is the minimum number of distinct points of the experimental sample and must not be confused with the sum of the numbers of points contained in a prescribed set of overlapping segments. Relation (29a) is a lower bound: a particular experimental sample may contain more points than this minimum. For $m_0 = m_1 = 0$ and $m_2 = 2$, for example, it gives $N \geq 11$; the parent-capacity requirement C ?C ²in (29) is therefore recovered exactly.

Information capacity and approximation accuracy have different functions. Insufficient information lowers the highest admissible class. Insufficient accuracy does not. If an information-admissible segment does not meet the prescribed accuracy but contains an interior experimental point that permits further multiplication, it retains its class and remains eligible for a subsequent greedy multiplication.

2.5 Phenotypic Identification for a Fixed Architecture

Once the boundaries, local classes, fundamental solutions, and boundary/contact conditions have been determined, the current architecture $\mathcal{A}$ is fixed. The corresponding composite spline can be written as

$$\sigma(\varepsilon; \mathbf{c}, \mathcal{A}) = \sum_{\alpha=1}^{n_{\mathcal{A}}} c_\alpha \, \phi_\alpha(\varepsilon; \mathcal{A}) \quad (30)$$

where ϕ_α belong to the variationally admissible space of the current architecture and c_α are its phenotypic coefficients.

The discrete part of the generalized principle is

$$\mathcal{D}(\mathbf{c} \mid \mathcal{A}) = \frac{1}{N} \sum_{k=1}^{N} [\sigma_k - \sigma(\varepsilon_k; \mathbf{c}, \mathcal{A})]^2 \quad (31)$$

The phenotypic coefficients are determined by

$$\mathbf{c}^*(\mathcal{A}) = \arg\min_{\mathbf{c}} \mathcal{D}(\mathbf{c} \mid \mathcal{A}) \quad (32)$$

subject to all boundary and contact conditions of the architecture. Thus,

$$\delta \mathcal{I} = 0 \Rightarrow \text{variationally admissible structure,}$$
$$\min_{\mathbf{c}} \mathcal{D} \Rightarrow \text{phenotypic realization of the structure.} \quad (33)$$

After every greedy multiplication, the architecture changes and problem (32) is solved in the new admissible solution space. This constitutes the hierarchical variational generalization of the Reinsch principle: variation within a fixed functional space is supplemented by discrete evolution of the admissible architectural space itself.

2.6 DOE as Variation of Spline Architecture and Structure

Sequential greedy multiplication generates a family of admissible architectures

$$\mathcal{A}_0, \mathcal{A}_1, \dots, \mathcal{A}_j, \dots, \tag{34}$$

with each transition produced by one local multiplication,

$$\mathcal{A}_j \to \mathcal{A}_{j+1} \tag{35}$$

In the present problem, DOE is applied to the successive architectural states generated by the deterministic Geometry Builder genealogy. The architectural state, rather than an arbitrarily prescribed numerical parameter set, is therefore the object to be registered, compared, and investigated. Symbolically,

$$\mathcal{A} = \{m; \varepsilon_1, \dots, \varepsilon_{m-1}; q_1, \dots, q_m; \mathcal{C}; \mathbf{c}\} \tag{36}$$

where $\mathcal{C}$ denotes the set of boundary and contact conditions.

For each structural state, phenotypic identification is performed first, after which its observable responses are evaluated:

$$\mathcal{A}_j \to \mathbf{c}^*(\mathcal{A}_j) \to \mathbf{R}_j = \mathbf{R}\left(\mathcal{A}_j, \mathbf{c}^*(\mathcal{A}_j)\right) \tag{37}$$

Thus, an individual DOE run corresponds not to an arbitrarily prescribed set of coefficients or to an independently selected point of a global architectural search space, but to one state of the deterministic genealogy together with its optimally identified phenotypic realization. DOE thereby acquires the new function

variation of architecture
→ phenotypic identification (38)
→ response evaluation

DOE does not replace greedy multiplication, does not generate the genealogy, and does not imply exhaustive enumeration or global optimization over all possible spline partitions and class compositions. Geometry Builder alone generates the admissible sequence of architectural states through the maximum-distance rule, information capacity, and variational conditions. DOE provides the formal framework for recording, comparing, and investigating the states and responses encountered along this deterministic genealogy. The global problem of searching for an optimal architecture outside this genealogy is not formulated or solved in the present work.

Together with structural stationarity and phenotypic minimization, this gives three levels of the hierarchical construction: the variational principle defines the admissible local structure; the discrete problem identifies the phenotype for each fixed state; and DOE organizes the investigation of the sequence of states generated by Geometry Builder.

Level I: $\delta\mathcal{I} = 0 \;\to$ variationally admissible structure,
Level II: $\min\mathcal{D} \;\to$ phenotypic coefficients, (39)
Level III: DOE $\to$ investigation of architecture and structure variations.

2.7 Dual Accuracy Control

For the phenotypic realization of the current architecture, two complementary error measures are used. The distributed discrepancy is characterized by the conventional vertical root-mean-square error

$$E_RMS = [(1/N)\ \Sigma_\{k = 1\}\hat{}N\ (\bar{\sigma}_k - S_m(\bar{\varepsilon}_k))^2]\hat{}\{1/2\} \tag{40}$$

$$D_max = max_k\ d_k \tag{41}$$

where d_k is the Euclidean point-to-curve distance defined by (15). Thus E_RMS characterizes the distributed vertical discrepancy, whereas D_max controls the strongest local geometric discrepancy and localizes the next multiplication. The prescribed accuracy is reached only when

$$E_RMS \le \delta_RMS, \qquad D_max \le \delta \tag{42}$$

If (42) is satisfied, the current architecture is accepted. If at least one inequality is violated, D_max also determines through (16) the location of the next structural change. The maximum Euclidean point-to-curve defect therefore has two roles: it is both a geometric accuracy measure and the localization

operator for the next multiplication. The two tolerances have different meanings: δ_RMS controls the auxiliary distributed-error measure, whereas δ is the prescribed geometric analysis resolution used for morphological selection.

2.8 Stopping Rule and Information Limit

After every accepted multiplication, the number of segments increases by one,

$$m_{j+1} = m_j + 1 \tag{43}$$

Accepted internal boundaries are neither removed nor relocated, and the experimental sample is not modified during construction. The genealogy of architectures is therefore monotone,

$$\mathcal{A}_0 \to \mathcal{A}_1 \to \cdots \to \mathcal{A}_m \tag{44}$$

If the dual criterion (42) is satisfied, construction terminates with the status

$$\text{ACCURACY REACHED} \tag{45}$$

If the required accuracy has not been reached but the segment containing the current global maximum Euclidean point-to-curve defect does not admit any further information-supported multiplication, further architectural refinement from the available sample is impossible. Construction terminates with the status

$$\text{INFORMATION LIMIT} \tag{46}$$

The last information-admissible architecture and its achieved error measures are retained. Geometry Builder therefore implements the sequence

$$\begin{gathered}\text{variational principle} \to \text{full-range model} \to \\ \text{phenotypic identification} \to \text{maximum} \\ \text{geometric defect} \to \\ \text{parent segment} \to \text{greedy multiplication} \to \\ \text{information-admissible child classes} \to \\ \text{new variational structure} \to \text{new phenotypic} \\ \text{identification} \to \text{accuracy control} \to \text{next} \\ \text{multiplication or stopping.}\end{gathered} \tag{47}$$

The terminal morphology

$$\mathcal{M} = \{m; \varepsilon_1, \dots, \varepsilon_{m-1}\} \tag{48}$$

is the geometric result of this sequential evolution of the architecture.

3. Theorem on Morphological Stability

Terminological note. The architecture of the interpolation template and the morphology of the deformation curve are strictly distinguished below. Architecture is the complete current computational state of the template: partition of the strain domain into segments, local smoothness classes, local polynomials and their coefficients, boundary and contact conditions, and the history of performed operations. Morphology is only the geometric result retained after Geometry Builder has completed: the number of segments and the coordinates of their internal boundaries. Therefore, different computational architectures—including architectures with different admissible sequences of local classes—may correspond to the same morphology, while a change in a local class or in polynomial coefficients with unchanged boundaries is not, by itself, a change in morphology.

Theorem (three-stage theorem on morphological stability). Let the working experimental sample be finite, the adaptive local-class rule $C^2 \to C^1 \to C^0$ and the information-admissibility rules be fixed, and the geometric and distributed-error tolerances be prescribed. Let each new internal boundary be introduced only at the experimental point of the current global maximum Euclidean point-to-curve defect. Then the Geometry Builder construction possesses the following three levels of morphological stability.

I. Finiteness and existence of a terminal morphology. Every accepted multiplication introduces one new internal boundary selected from the finite working sample. No accepted boundary is subsequently removed or relocated, and the working sample is not smoothed. Hence the number of admissible multiplications is finite. After a finite number of steps Geometry Builder therefore either satisfies the dual accuracy criterion or reaches the information limit because no further information-admissible split is possible. In either case a finite terminal morphology and an explicit stopping status exist.

II. Local stability of morphology. Suppose that, for

the terminal result, all inequalities determining the construction are strict: at every accepted step the global maximum Euclidean point-to-curve defect is separated from competing defects by a nonzero margin, the information-admissibility decisions are unchanged, and the terminal error measures are separated from the prescribed accuracy thresholds whenever the corresponding comparison is active. Then there exists a sufficiently small neighborhood of perturbations of the working sample and accuracy parameters within which the sequence of selected split indices and local-class decisions remains unchanged. In this neighborhood, the structural morphology is preserved—the number of segments and the correspondence of internal boundaries to the same sample indices. Under continuous changes in the coordinates of experimental points, the boundary coordinates themselves vary continuously. Thus, local morphological stability includes both structural stability of the segmentation and coordinate stability of its boundaries.

III. Boundary of morphological stability and discrete transition. Morphology can change only when a determining comparison loses its strict margin: two or more Euclidean point-to-curve defects exchange the role of global maximum; an information-admissibility threshold is crossed and thereby changes a subsequent split decision; or an accuracy threshold is crossed, changing the stopping decision. Upon crossing such a boundary, a continuously small change in the source data or accuracy parameters may produce a discrete change in the sequence of split indices or in the number of segments and hence a transition to another admissible morphology. A change in local smoothness class with the number and coordinates of segment boundaries preserved changes the architecture, but not the morphology. Such transitions are not a loss of algorithmic determinacy; they are boundaries between piecewise-stable outcomes of the deterministic genealogy.

Proof. The first stage follows directly from finiteness of the working sample and monotonicity of the construction: each accepted operation adds one boundary and no operation removes, relocates, or reverses an accepted split. The second stage follows from stability of strict inequalities under sufficiently small perturbations. As long as the ordering of Euclidean point-to-curve defects, the information-admissibility decisions, and the stopping comparisons remain unchanged, the same sequence of sample indices is selected as boundaries. Continuity of the local interpolation constructions with respect to the sample coordinates then implies continuous shifts of the corresponding boundary coordinates. The third stage is the complement of the second: a structural transition requires at least one determining margin to vanish and the associated discrete decision to change. Thus, morphology is a piecewise-stable function of the experimental sample and accuracy parameters, and the decision-equality surfaces form the boundaries of the regions of morphological stability. This completes the proof.

Corollary. Morphology is not an a priori prescribed architecture of the interpolation template. It is a stable geometric result of the computational construction within a region of morphological stability. Therefore, its structural stability is assessed by preservation of the number of segments and the index localization of their boundaries, whereas coordinate stability is assessed by the smallness of boundary-coordinate shifts under small perturbations of the working sample and accuracy parameters; stability of the coefficients of local quintic polynomials is not, by itself, a criterion of morphological stability.

4. Numerical Examples

The numerical experiments were designed to verify the geometric mechanism of morphology formation independently of the subsequent physical identification problem. Three original experimental samples with substantially different deformation-curve geometries were selected: 1018 steel, BT6 titanium alloy, and A201.0-T7 aluminum alloy. For all three materials, the

same Geometry Builder implementation, the same six-stage preprocessing procedure for the experimental sample, the same variational hierarchy $C^2 \to C^1 \to C^0$, and the same mandatory geometric split rule were used. The preprocessing procedure comprises validation, strain sorting, deduplication, retention of the loading branch through the first global stress maximum, zero-offset calibration of both strain and stress, and normalization. No number of segments or internal-boundary coordinates was prescribed in advance.

4.1 Preprocessing and Geometric Accuracy Measure

The source sample is first validated, sorted by strain, and deduplicated. The loading branch is retained up to and including the first global maximum of stress. Let ε_0 and σ_0 denote the strain and stress recorded at the first accepted point of this branch. Zero-offset calibration of the measuring system is then performed by translating the working sample by these initial readings in both coordinates. The calibrated branch is subsequently normalized by its accepted strain and stress ranges. The source data are not modified; all transformations are applied only to the working copy.

$$\varepsilon^c = \varepsilon - \varepsilon^0, \qquad \sigma^c = \sigma - \sigma^0 \tag{49}$$

$$\bar{\varepsilon} = (\varepsilon - \varepsilon_0)/(\varepsilon_max - \varepsilon_0), \qquad \bar{\sigma} = (\sigma - \sigma_0)/(\sigma_max - \sigma_0) \tag{50}$$

For a sample point $P_i=(\bar{\varepsilon}_i,\bar{\sigma}_i)$ and the current spline S_m containing m segments, the governing local discrepancy is the Euclidean point-to-curve distance d_i defined by (15). In the implemented genealogical construction the distance is evaluated on the current local spline segment containing the abscissa of the sample point; this preserves an unambiguous parent segment for the next multiplication. Accordingly,

$$d_i = d(P_i, S_\{j(i)\}) \tag{51}$$

$$D_max\^\{(m)\} = max_i \;\; d_i \tag{52}$$

The point attaining D_max determines both the parent segment and the mandatory position of the next internal boundary. The conventional vertical root-mean-square error defined by (40) is retained only as an auxiliary distributed-error characteristic; for the m-segment state we write

$$E_RMS\^\{(m)\} = E_RMS(S_m) \tag{53}$$

Thus, D_max is the primary geometric quantity controlling the localization of morphological refinement, whereas E_RMS is reported as a complementary global measure. The numerical experiment does not use an a priori prescribed segment number. For a selected geometric analysis resolution δ, the first genealogical state whose maximum Euclidean point-to-curve defect is below δ is identified, subject also to the independently prescribed auxiliary tolerance δ_RMS. These tolerances must not be conflated.

$$m * (\delta) = min\{m: \; E_RMS\^\{(m)\} \le \delta_RMS, \; D_max\^\{(m)\} \le \delta\} \tag{54}$$

The quantity m*(δ) is therefore not claimed to be a global optimum over all conceivable spline partitions. It is the least complex experimentally admissible state on the deterministic genealogy generated by Geometry Builder for the prescribed geometric analysis resolution δ and the fixed auxiliary tolerance δ_RMS. The natural scale δ_sample = 1 / (N - 1), introduced below for each normalized working sample, characterizes only its discrete sampling density and is not substituted for δ except when that particular comparison is intentionally made. This distinction is essential because global reidentification of the phenotypic coefficients after a split can make the error history locally nonmonotone.

4.2 Numerical Experiment for 1018 Steel

After preprocessing, the working sample of 1018 steel contains N = 209 points. The natural normalized sampling scale δ_sample = 1 / (N - 1) is 0.00480769. The full-range C^2 model gives a large geometric discrepancy and is successively multiplied at mandatory maximum-distance points. The experimentally admissible morphology changes stepwise as δ decreases. In the representative range investigated here the first admissible states are m = 3 for δ = 0.03, m = 5 for δ = 0.025-0.015, m = 8 for δ = 0.01, and m = 14 for δ = δ_sample = 1 / (N - 1) ≈ 0.00481.

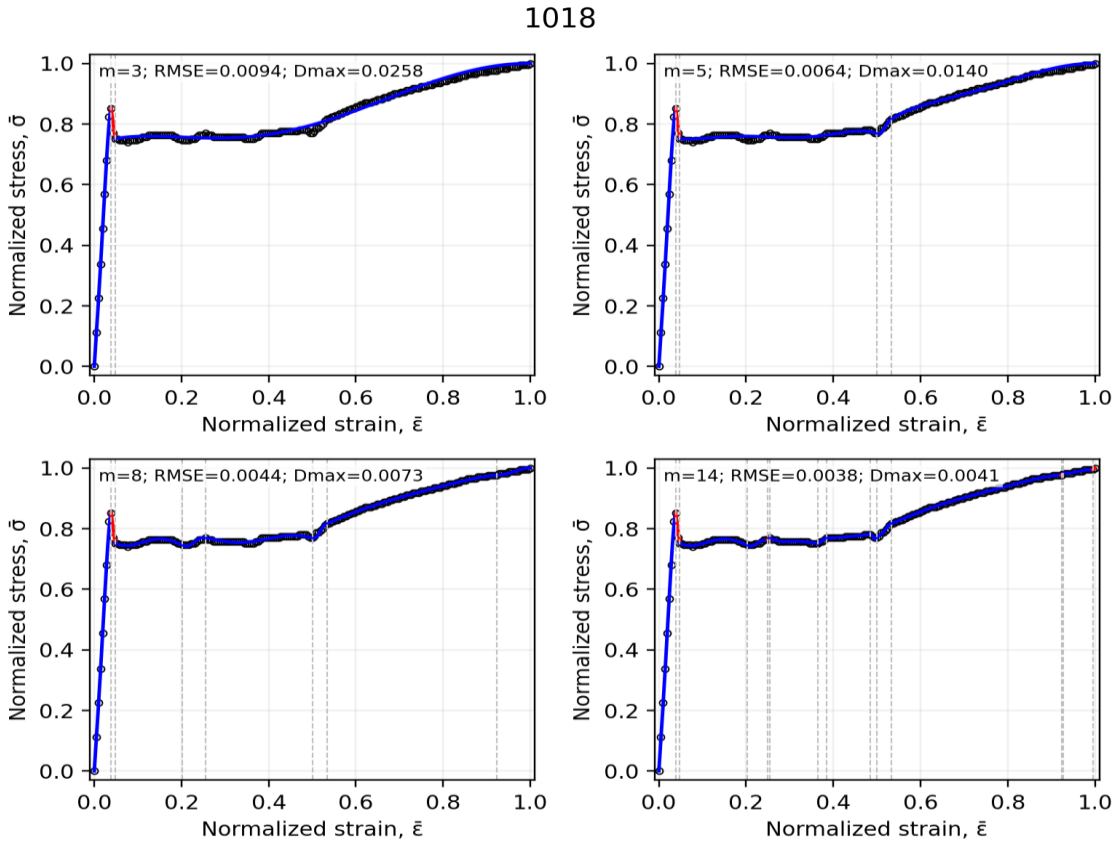


Fig. 1 Sequential segmentation of 1018 steel for decreasing experimental resolution δ. Experimental points are shown by circles; linear C^0 segments are red and nonlinear C^1/C^2 segments are blue. Dashed vertical lines mark accepted internal boundaries. The panels show representative first-admissible states of the Geometry Builder genealogy.

The 1018 sequence also demonstrates that the genealogy itself is not an error-monotone sequence. The four-segment state is worse than the preceding three-segment state in both reported measures, and the six-segment state has a slightly larger D_max than the five-segment state. Consequently, intermediate architectures may be bypassed when the first state satisfying a prescribed δ is selected. The resulting morphology is therefore a stepwise function of experimental resolution rather than a direct function of the iteration number.

4.3 Numerical Experiment for BT6

For BT6, the preprocessed working sample contains N = 158 points and δ_sample = 1 / (N - 1) = 0.00637. The two-segment C ⁷C ²state gives E_RMS = 0.02414 and D_max = 0.04658 and is the first admissible state at δ = 0.05. For δ = 0.04-0.0125 the first admissible state contains three C ² segments, with E_RMS = 0.00865 and D_max = 0.01247. Tightening the resolution to δ = 0.01-0.005 gives a four-segment C ⁷C ⁷C ⁷C ²morphology with E_RMS = 0.00209 and D_max = 0.00482. At δ = 0.003, the first admissible state contains fourteen segments because the prescribed resolution approaches the local geometric scale of this dense experimental curve.

The BT6 result is important because it shows that the stepwise mechanism observed for 1018 is not tied to a particular deformation-curve shape. At the same normalized experimental resolution, BT6 can require substantially fewer segments than 1018. The response m*(δ) is therefore material-specific even when the construction rule and the resolution parameter are common.

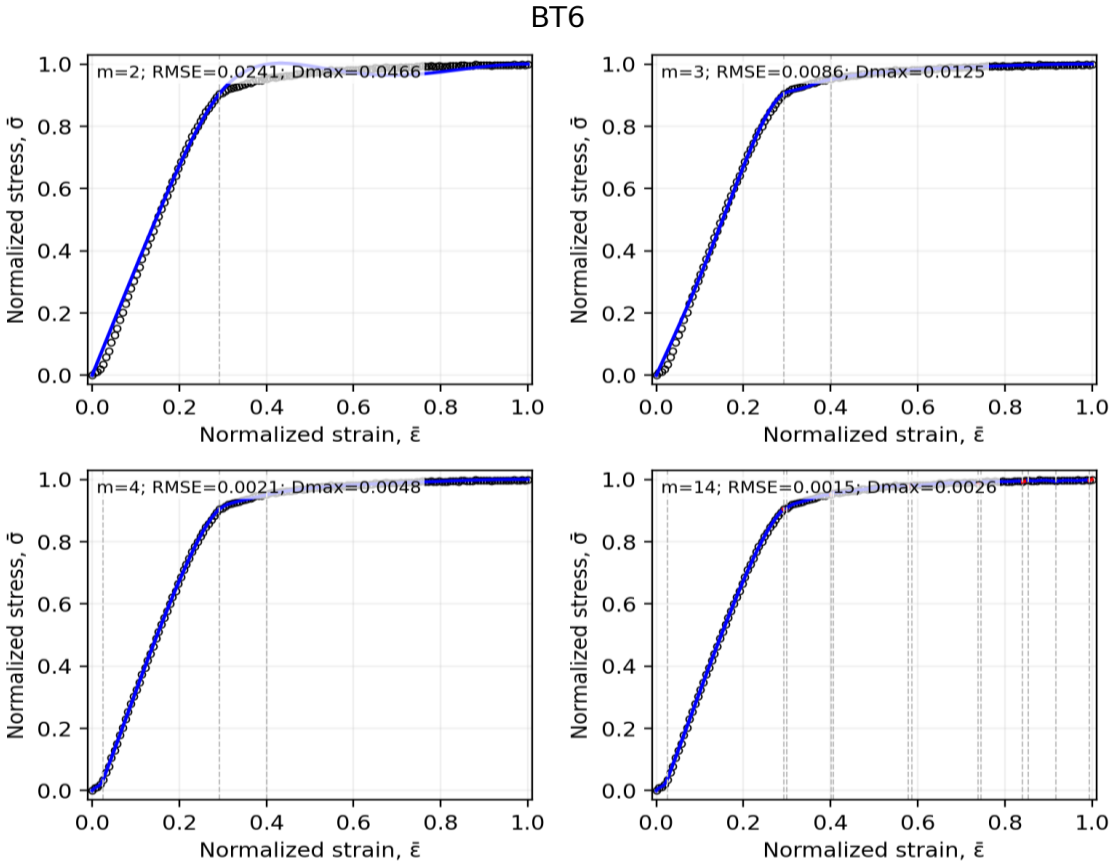


Fig. 2 Sequential segmentation of BT6. The same plotting convention and Geometry Builder rules as in Fig. 1 are used. Representative first-admissible states contain 2, 3, 4, and 14 segments as the prescribed resolution is tightened.

4.4 Numerical Experiment for A201.0-T7

For A201.0-T7, the preprocessed working sample contains N = 280 points, giving δ_sample = 1 / (N - 1) = 0.00358. The two-segment C ⁷C ²state has E_RMS = 0.00358 and D_max = 0.00885 and is already admissible for $\delta \geq 0.01$. At δ = 0.0075-0.005, the first admissible state contains three C ² segments, with E_RMS = 0.00267 and D_max = 0.00461. At δ = 0.003 the first admissible state contains nine segments. Thus the same reduction of δ produces a different segmentation sequence from both 1018 and BT6.

This example again shows that the experimentally sufficient architecture is selected by the attained discrepancy rather than by segment count alone. The two-segment morphology remains sufficient over a wide resolution interval, the three-segment morphology appears only after δ falls below 0.00885, and substantially finer segmentation is required only when δ approaches 0.003.

4.5 Comparison of the Three Materials

The three experiments produce different staircases of experimentally admissible morphologies under the same deterministic construction. In the investigated resolution ranges, the representative transitions are 3→5→8→14 for 1018, 2→3→4→14 for BT6, and 2→3→9 for A201.0-T7. The common feature is not a universal segment number but the discrete nature of the response: continuous tightening of the experimental resolution produces piecewise-constant morphology separated by discrete structural transitions.

$$\delta \downarrow \quad \Rightarrow \quad m_{\mathrm{opt}}(\delta) \text{ changes by discrete genealogical transitions} \tag{55}$$

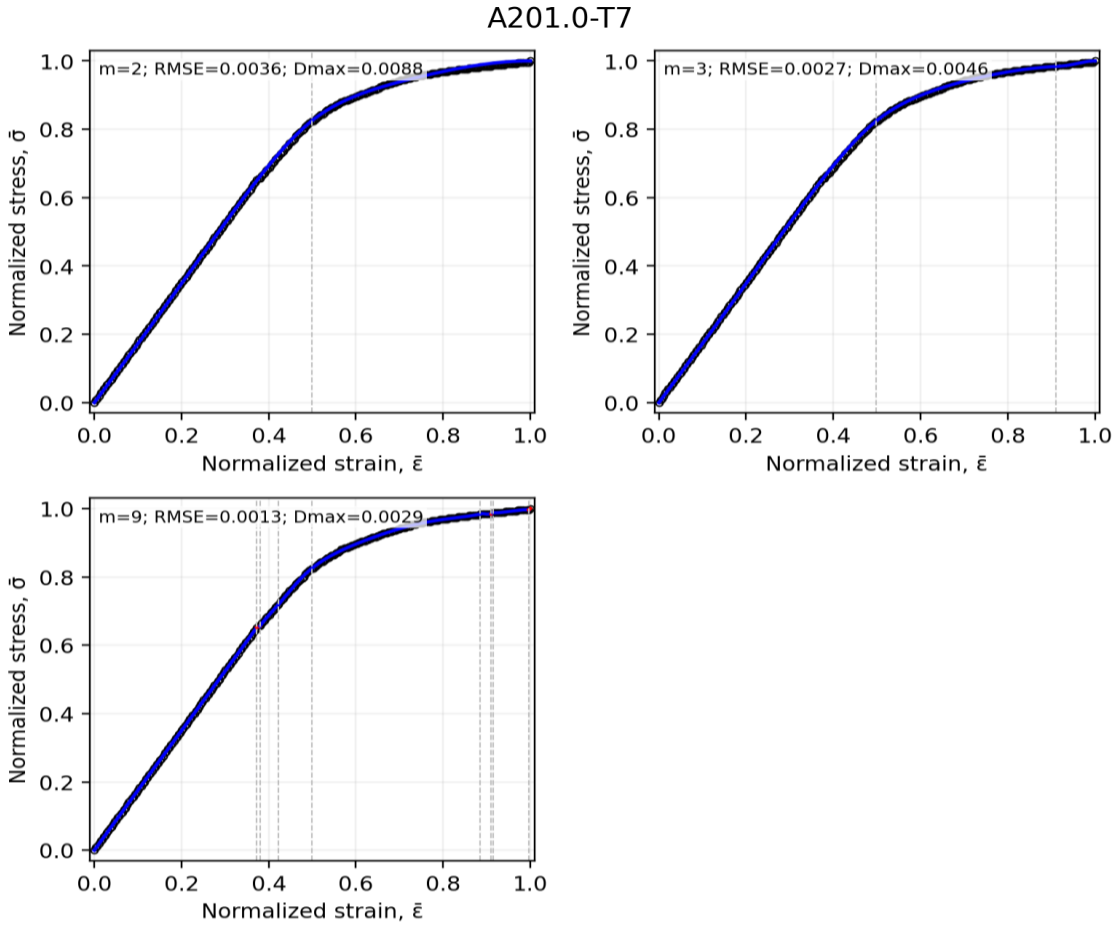


Fig. 3 Sequential segmentation of A201.0-T7. Representative first-admissible states contain 2, 3, and 9 segments as the prescribed resolution is tightened.

For BT6 the minimum pairwise distance in the normalized plane is 0.00600, close to the natural sampling scale δ_sample = 1 / (N - 1) = 0.00637. For A201.0-T7 the corresponding values are 0.0035806 and δ_sample = 0.0035842. For 1018 the working sample contains 209 points and the minimum pairwise distance is approximately 0.00480769, again close to δ_sample = 1 / (N - 1). This repeated numerical proximity is reported only as an empirical observation for the present samples; δ_sample is a property of the discrete working sample and is not the prescribed analysis resolution δ, nor is it used as a general theorem or a universal stopping rule.

At the common resolution δ = 0.0125, BT6 requires three segments whereas A201.0-T7 is already represented by two. The comparison directly demonstrates that the same experimental resolving scale produces different morphological complexity for different materials. Morphology is therefore determined jointly by the geometry of the material response and by the resolution at which that geometry is observed.

4.6 Numerical Interpretation of the Stopping Rule

The calculations support a restrained interpretation of architectural optimality appropriate to the geometric scope of the present paper. Geometry Builder does not solve a global combinatorial optimization over all possible partitions. It constructs one deterministic genealogy by mandatory multiplication at the largest current Euclidean point-to-curve defect. Within this genealogy, the experimentally sufficient morphology is the first state indistinguishable from the sample at the prescribed resolution δ.

$$m_{\mathrm{opt}}(\delta) = \min\{m:\ A_m \text{ is admissible at resolution } \delta\} \quad (56)$$

This definition separates the result established here from the broader problem of analytical optimization of spline architecture. The latter requires comparison of alternative architectural realizations and belongs naturally to the subsequent stages of physical identification and computational platform development. For the present geometric problem, the numerical evidence is sufficient to establish three facts: morphology is generated rather than prescribed; its experimentally sufficient complexity changes discretely with resolution; and the resulting staircase is material-specific.

5. Conclusion

A hierarchical variational generalization of the Reinsch principle has been proposed for constructing an adaptive interpolation-spline architecture from a finite sample of experimental points of the deformation curve of an elastoplastic material. In contrast to the traditional formulation, in which the structure of the approximating function is assumed to be prescribed, the present construction separates the variational determination of the spline structure, the identification of its phenotypic coefficients, and the successive modification of the architecture itself.

Stationarity of the integral part of the variational functional determines, for each local class C^q, the corresponding space of fundamental solutions together with a variationally consistent system of boundary and contact conditions. For the C^0, C^1, and C^2 classes, this unified construction leads respectively to linear, cubic, and quintic local solutions. The discrete part of the problem performs a different function: for a fixed architecture, its minimum determines the phenotypic coefficients of the local fundamental solutions that provide the best reproduction of the experimental sample.

The starting basis for the genealogical construction is the full-range model, a single C^2 segment spanning the entire normalized strain domain. If the attained accuracy is insufficient, the architecture develops through greedy multiplication. The parent is the segment containing the experimental point of the global maximum Euclidean point-to-curve defect; the same point becomes the mandatory new internal boundary and the common experimental point of the two child segments. Multiplication is local and includes four structurally distinct cases: multiplication of the full-range model, an internal parent, a left-end parent, and a right-end parent. Previously accepted boundaries are neither removed nor relocated.

The class of each newly created segment is determined independently of its current approximation error as the highest class admissible by its information capacity. Information sufficiency and accuracy of reproduction of the experimental sample are therefore strictly separated: insufficient information causes the transition $C^2 \to C^1 \to C^0$, whereas insufficient accuracy in the presence of sufficient information leads not to class reduction but to subsequent multiplication of the corresponding segment. Construction terminates either when the root-mean-square and maximum Euclidean point-to-curve defect criteria are simultaneously satisfied or when the information limit is reached.

For a terminal architecture with m_0, m_1, and m_2 segments of classes C^0, C^1, and C^2, this local information hierarchy yields the global lower estimate $N \geq m_0 + 3m_1 + 5m_2 + 1$ for the number of distinct experimental sample points. This estimate characterizes information sufficiency of the architecture and is independent of the subsequent physical identification problem.

This construction gives DOE a new but deliberately restricted function. DOE is used to organize and compare the successive architectural states produced by the deterministic Geometry Builder genealogy. Each such state has its own optimally identified phenotypic realization and corresponding computed responses. The variational principle establishes the mathematical admissibility of the local structures, Geometry Builder

determines the genealogy, and DOE systematizes the investigation of the states actually generated along it. No exhaustive or global search for an optimal architecture is performed in the present work.

The proposed construction therefore comprises three mutually connected levels: variational stationarity defines the admissible structure; minimization of the discrete part determines the phenotypic coefficients; and DOE organizes investigation of the deterministic genealogy generated by Geometry Builder. The final geometric result of this hierarchical procedure is the morphology of the deformation curve, defined solely by the number of segments and the coordinates of their internal boundaries. Morphology is not prescribed in advance and does not include local classes or phenotypic coefficients; it emerges from the successive evolution of the architecture from the full-range model to a state that either satisfies the prescribed accuracy or is limited by the information capacity of the experimental sample.

Thus, the result extends beyond an algorithm for automatic placement of spline knots. It provides a unified variational-computational representation of the sequence full-range model → greedy multiplication → deterministic genealogy of adaptive architectures → DOE-based comparison of generated states → morphology. The present paper deliberately stops at this deterministic genealogical construction and does not formulate a global optimization over the full space of possible architectures. The resulting morphology is an independent geometric result and simultaneously forms a fixed geometric basis for the next stage of genetic identification: construction of an approximation template and determination of the physical parameters of the material through the additional Platform module, Material Builder. This explicitly establishes the continuation of the present work toward further development of the Platform and subsequent machine recognition of elastoplastic materials.

References

[1] Belov, P. A. 2026. “Foundations of the Genetics of Elastoplastic Materials.” *Journal of Civil Engineering and Architecture* 20: 129-46. doi:10.17265/1934-7359/2026.04.001.

[2] Belov, P. A., and Golovina, N. Ya. 2026. “Structural Theory of Elastoplastic Material Models.” *Journal of Civil Engineering and Architecture* 20: 281-91. doi:10.17265/1934-7359/2026.07.003.

[3] Belov, P. A., and Weiss, E. 2026. “Direct and First Inverse Problems of Genetic Identification of Materials at a Fixed Smoothness Class.” *Journal of Civil Engineering and Architecture* 20: 322-39. doi:10.17265/1934-7359/2026.08.002.

[4] Belov, P. A., and Weiss, E. 2026. “The Second Inverse Problem of Genetic Identification of Materials: Selection of the Optimal Model Architecture.” *Journal of Civil Engineering and Architecture* 20: 347-58. doi:10.17265/1934-7359/2026.08.004.

[5] Reinsch, C. H. 1967. “Smoothing by Spline Functions.” *Numerische Mathematik* 10 (3): 177-83. doi:10.1007/BF02162161.